Analyst

PAPER

View Article Online
View Journal | View Issue

Cite this: *Analyst*, 2016, **141**, 5382

Use of aminothiophenol as an indicator for the analysis of silver nanoparticles in consumer products by surface-enhanced Raman spectroscopy†

Trang H. D. Nguyen,[a] Peng Zhou,[b] Azlin Mustapha[a] and Mengshi Lin*[a]

Received 11th April 2016,
Accepted 14th June 2016

DOI: 10.1039/c6an00835f

www.rsc.org/analyst

Silver nanoparticles (Ag NPs) are one of the top five engineered nanoparticles that have been used in various products. Current methods for the measurement of Ag NPs are time consuming and expensive. Therefore, it is of critical importance to develop novel strategies to detect the presence of Ag NPs at low concentrations in different matrices. This study aimed at detecting and measuring Ag NPs in consumer products using surface-enhanced Raman spectroscopy (SERS) coupled with aminothiophenol (PATP) as an indicator molecule that binds strongly with Ag NPs. Quantification and qualification of Ag NPs were achieved using this method of acquiring SERS signals from Ag NP–PATP complexes. Four dietary supplement products and one nasal spray were selected to evaluate the performance of SERS in the detection of Ag NPs. Inductively coupled plasma optical emission spectrometry (ICP-OES) and transmission electron microscopy (TEM) were utilized to measure the physical properties of Ag NPs in the samples. The results demonstrate that distinctive Raman peaks of PATP can be used to distinguish Ag NPs from silver bulk particles and silver nitrate. SERS is able to detect Ag NPs with different sizes ranging from 20 to 100 nm, with the highest intensity for ~30 nm Ag NPs. A partial least squares method was used to develop quantitative models for the analysis of spectral data (R = 0.94). These results indicate that the conjugation of Ag NPs with PATP can be measured by SERS. These results demonstrate that SERS is a simple and rapid method and has great potential to detect Ag NPs in various products.

Introduction

Engineered nanoparticles (ENPs) have received much attention in recent years due to their unique properties that are applicable for use in nanosensors, pathogen detection, and antimicrobial application.[1] For example, metal oxide nanoparticles have been used as antimicrobial agents that can inhibit the growth of microorganisms.[2,3] Nanoparticle-based sensors can provide a platform to detect microbes, pesticides, or chemical contaminants in complex matrices.[1,4,5] Among various ENPs, silver nanoparticles (Ag NPs) are one of the top five nanoparticles widely used in pharmaceutical products, building materials, and consumer products.[6–9] Around 24% of commercial nano-based products claimed to contain Ag NPs.[10] Ag NPs have been found in various products, ranging from textiles, dietary supplements, cosmetics, household products, cleaning agents, medical supplies such as nasal sprays and top cream brands, and antimicrobial food packaging materials because of their exceptional ability to inhibit bacterial growth.[2,11,12]

With increasing applications of Ag NPs, some concerns have been raised about their risks and potential negative effects on human health.[13] Recent studies show that Ag NPs may enter the human body *via* different routes, potentially damage various internal organs and cause serious human diseases.[14,15] To measure Ag NPs in various products and fully understand the effects of NPs on human health, it is of critical importance to develop suitable techniques to detect Ag NPs that are usually present at low concentrations in various matrices.

Current analytical methods for the detection, characterization and quantification of Ag NPs include scanning electron microscopy (SEM), transmission electron microscopy (TEM), and energy dispersive X-ray spectroscopy (EDS). These techniques have been widely used to characterize the size, shape, elemental composition, and surface morphology of NPs. For example, Lozano and others (2012) employed EDS to quantify engineered Ag NPs in coffee, milk, and water.[16] Inductively coupled plasma optical emission spectrometry (ICP-OES) or

[a]*Food Science Program, Division of Food Systems & Bioengineering, University of Missouri, Columbia, MO, 65211-5160 USA. E-mail: linme@missouri.edu*
[b]*School of Food Science and Technology, Jiangnan University, Wuxi, Jiangsu, 214122 China*

†Electronic supplementary information (ESI) available. See DOI: 10.1039/c6an00835f

inductively coupled plasma mass spectrometry (ICP-MS) has been used to determine metal NPs in agricultural and food samples.[17–19] Single particle ICP-MS (SP-ICP-MS) can be used to differentiate between whole nanoparticles in matrices and their solvated residual ions.[20] Our previous study used TEM, SEM, EDS, and ICP-OES for the detection of Ag NP contamination in pears.[21] Dynamic light scattering (DLS) has been used for the detection of inorganic engineered nanomaterials,[22] or coupled with matrix-assisted laser desorption/ionization-time-of-flight (MALDI-TOF) mass spectrometry and hydrodynamic chromatography (HDC) to separate nanoscale liposomes from an orange-flavored beverage.[23] However, these characterization methods are time-consuming and labor-intensive. They often require complicated procedures for sample pretreatment and well-trained personnel to operate complex equipment. ICP-OES or ICP-MS measures the total silver content, but provides no information on the particle size or other properties.[24] Therefore, there remains a need to develop simple, rapid, sensitive, and non-destructive alternative methods for the detection of Ag NPs in various products.

Surface-enhanced Raman spectroscopy (SERS) is a novel technique that has received much attention in analytical chemistry, materials science, food safety, and other areas in recent years.[25] SERS is a branch of Raman spectroscopy in which probed molecules are adsorbed onto the roughened surface of noble metals, resulting in significant enhancement of the Raman signals. SERS is able to detect trace amounts of analyte molecules with potential to detect a single molecule or a single cell.[26–28] SERS has been increasingly applied for the detection of chemical adulterants or contaminants such as melamine, veterinary drugs, and pesticides in foods and other products.[25,29–31] Two enhancement mechanisms of SERS are widely accepted: electromagnetic enhancement (EM) and chemical enhancement, in which the EM mechanism makes a major contribution to the enhancement of Raman scattering.

Most previous SERS studies were focused on using gold or silver as a substrate to detect various analytes. However, in this study we investigated the feasibility of using SERS to detect Ag NPs in complex matrices using 4-aminothiophenol (*p*-aminothiophenol, PATP) as a Raman reporter. PATP is an aromatic thiol that has been found to be an ideal molecule for SERS analysis. PATP can strongly interact with metallic SERS substrates and produce very strong SERS signals.[32–36] PATP is a molecule that has been used to study the photon-driven charge transfer mechanism of SERS.[33] To the best of our knowledge, this is the first study to use SERS coupled with PATP as an indicator for detecting Ag NPs in commercial products. Additionally, TEM and ICP-OES were used to evaluate the capacity of the SERS method for the determination of Ag NPs.

Materials and methods

Materials

Ethanol (≥99.5%), $AgNO_3$ (99.8%), and 4-aminothiophenol (PATP) were all purchased from Sigma-Aldrich (St Louis, MO, USA). Methanol (99%) and nitric acid were purchased from Fisher Scientific (Pittsburgh, PA, USA). Spherical Ag powder with a diameter of 0.5–1 μm (99.9%) was purchased from Alfa Aesar (Ward Hill, MA, USA). Citrate-capped Ag NP colloids with diameters of 20, 30, 60, or 100 nm and a mass concentration of 20 mg L^{-1} were purchased from NanoComposix (San Diego, CA, USA). Five commercial products that claimed to contain Ag NPs were purchased from Walgreens and Amazon. Additional information about these products is listed below.

(a) A dietary supplement whose label lists 96% positively charged silver particles (10 ppm);

(b) a nasal spray that claims to contain 30 ppm of pure colloidal silver;

(c) a dietary supplement whose label lists pure nano silver particles suspended at 50 ppm in distilled water;

(d) a mineral supplement which lists purified silver of 30 ppm and purified water as the ingredients;

(e) a dietary supplement that claims to contain 10 ppm of nano colloidal sliver.

We use "S1–S5" to represent these products according to the (a)–(e) order above.

Characterization of Ag NPs in the products

An aliquot of Ag NP suspension sample (10 μL) was directly placed onto copper/carbon 200 mesh grids, air dried in a laminar flow hood for ~3 h, and then analyzed by using a JEOL 1400 (JEOL Ltd, Tokyo, Japan).

Determination of Ag NPs in tested products

The total silver content in each product was measured by ICP-OES (Varian Vista-MPX CCD Simultaneous ICP-OES, Walnut Creek, CA, USA). Before measurement, a volume of 10 mL of sample was acid-digested with 10 mL HNO_3 (Fisher Scientific, ACS Reagent) in a microwave digester. The digested samples were diluted with DI water to 50 mL, and then filtered before subjecting to the ICP-OES measurement.

To determine the presence of Ag NPs, it is necessary to separate Ag NPs from silver ions. All the samples were diluted 1 : 10 with Mill-Q water and filtered through 0.2 μm (25 mm diameter) sterile Millex® filters (Merck Millipore, Darmstadt, Germany) to separate particles smaller than 200 nm from larger particles in select samples. A 3 kDa-cutoff centrifuge filtering unit (Millipore Amicon Ultra-15, at 3578*g*, 30 min) was used to isolate Ag NPs from ionic silver. The filtrates were collected and digested using the aforementioned method before being subjected to ICP-OES measurement.

Conjugation of PATP onto Ag NPs

Conjugates of Ag NPs and PATP were prepared *via* thiol groups of PATP and Ag NPs. Briefly, Ag NP solutions (20 mg L^{-1}) were mixed with 10 mg L^{-1} PATP (volume ratios of 3 : 17). The mixture was incubated in a mixer (Max Mix II 37600, Thermolyne, Fisher Scientific) for 1 h at room temperature. The solution was then centrifuged for 5 min at 3915*g* to concentrate the Ag NP–PATP complexes at the bottom of the

centrifuge tube. The aggregation was then deposited onto a gold slide for air drying in a fume hood. PATP alone was used as a blank control while a mixture of PATP and $AgNO_3$ (20 mg L^{-1}) was considered as a negative and a positive control, respectively. In addition, the five commercial products were amended with PATP using the method described above.

Detection of Ag NPs using SERS and Ag NP–PATP conjugation

The samples on a gold slide were immediately analyzed by a Renishaw RM1000 Raman Spectrometer System (Gloucestershire, UK) equipped with a Leica DMLB microscope (Wetzlar, Germany) and a 785 nm near-infrared diode laser source. During the measurement, light from a high power diode laser was directed and focused onto the sample on a microscope stage through an objective. Raman scattering signals were detected by using a 578 × 385 pixels charge-coupled device array detector. The WiRE 3.4 software (Gloucestershire, UK) was used to collect spectral data. In this study, the spectra of samples were collected using a ×50 objective with 10 s exposure time, 0% focus, and ~20 mW laser power in the extended mode. Detection ranges for each sample were 400–1800 cm^{-1} for all the measurements.

Data analysis

The software Delight version 3.2.1 (D-Squared Inc., LaGrande, OR, USA) was used for data analysis. Eight locations in each sample were randomly measured and averaged to obtain a final spectrum, which was then compared across all sample treatments. In this study, the analysis of SERS spectral data was based on our previously published methods.[37] Briefly, a polynomial subtract was employed to adjust the baseline shift. In this study, the multivariate statistical analysis was performed using the partial least squares (PLS) method coupled with the leave-one-out (LOO) cross-validation algorithm. The PLS model was established to predict Ag NP concentrations in tested samples. LOO cross-validation was used to evaluate the quality of the model.[38,39] In this method, $(n-1)$ samples were used to build a calibration model. Each sample in the data set was eventually used for this loop procedure. In this way, the cross-validation acts as LOO on the whole samples. The predicted analyte concentrations (Ag NPs) in tested samples were calculated based on correlations between spectral features and chemical reference values and then compared with the reference values.

The number of PLS latent variables was optimized based on the lowest root mean square error of prediction (RMSEP) values to avoid over-fitting of spectral data. The spectral data were smoothed with a Gaussian function at 4 cm^{-1} followed by a second derivative transformation with a 12 cm^{-1} gap before the PLS was conducted. The correlation coefficient (R) and RMSEP were used to evaluate the model based on the R value or the RMSEP value. Normally, the higher the R value is, the better predictability the model has.

The limit of detection (LOD) with a 99.86% confidence interval can be calculated from the PLS calibration curve based on characteristic peaks in SERS spectra using the following formula:

$$\mathrm{LOD} = 3\sigma/m$$

in which σ is the standard error of the predicted concentration, and m is the slope of the calibration curve. In a PLS model, σ equals to RMSEP.[40]

Results and discussion

Effectiveness of SERS to characterize and quantify Ag NPs

Fig. 1 shows the SERS spectra of PATP, PATP mixed with $AgNO_3$ or silver powder with a size of 0.5–1 μm, and PATP mixed with 30 nm Ag NPs. It can be observed that only Ag NP–PATP complexes generated significantly enhanced Raman signals, whereas PATP alone yielded very weak Raman signals. This was due to the electromagnetic enhancement and the chemical enhancement produced by the charge transfer between Ag NPs and PATP through the Ag–S bond. Several prominent peaks can be observed, such as ν(CS) at 1078 cm^{-1} (a_1 mode), and b_2 mode (in-plane, and out-of-plane modes) located at 1590, 1435 and 1143 cm^{-1}. The apparent enhancement of the b_2 mode has been ascribed to the charge transfer of the metal to the adsorbed molecules and demonstrates that PATP adopts a perpendicular orientation to the metal surface.[36] A similar SERS characteristic pattern of PATP was also observed in other previous studies.[32–34,36] Interestingly, $AgNO_3$ and silver bulk materials provided no enhancement to the Raman signals of PATP, indicating that only nanoparticle-specific reactions occurred between Ag NPs and PATP. This method can be used to distinguish Ag NPs from other silver species.

Effect of different sizes of Ag NPs on the SERS enhancement

Four different sizes of Ag NPs (20, 30, 60, and 100 nm) were used to evaluate the feasibility of SERS to detect Ag NPs (Fig. 2). For 20 and 30 nm Ag NPs, strong and consistent

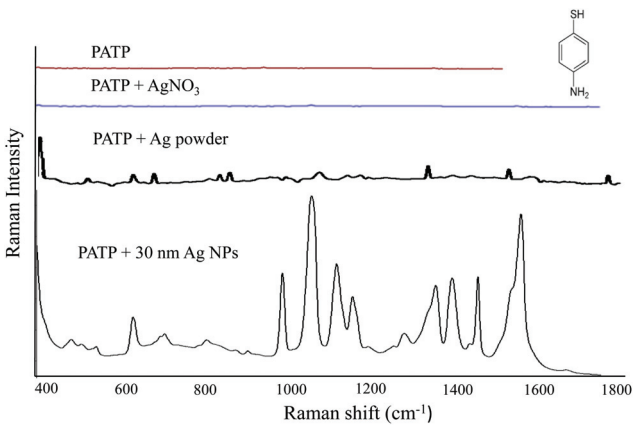

Fig. 1 SERS spectra of PATP, PATP mixed with $AgNO_3$, Ag powder (0.5–1 μm), and PATP with 30 nm Ag NPs.

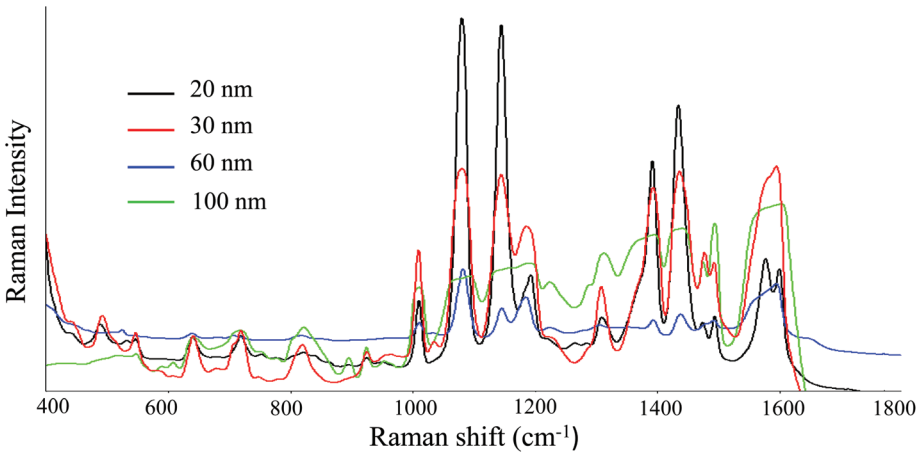

Fig. 2 SERS spectra of the conjugates of PATP with different sizes (20, 30, 60, and 100 nm) of Ag NPs.

SERS signals of PATP were obtained exhibiting excellent specific vibrational modes of PATP. However, the signal intensity and sharpness of characteristic peaks began to decrease with the increase of the particle size (Fig. 2). It is noteworthy that the SERS spectra of PATP with 100 nm Ag NPs exhibited broadened peaks. This phenomenon can be explained by the size dependent excitation of Ag NPs. SERS-active systems must ideally possess a structure in the 5–100 nm range.[41] Seney *et al.* found that as the particle size increases, SERS activities decrease. The 15 nm Ag NPs have the strongest SERS activity.[42] For the large size fraction of Ag particles (0.5–1 μm), little or no SERS response was observed (Fig. 1). Furthermore, Ag NPs that were arranged closely to one another could produce more intense electromag-

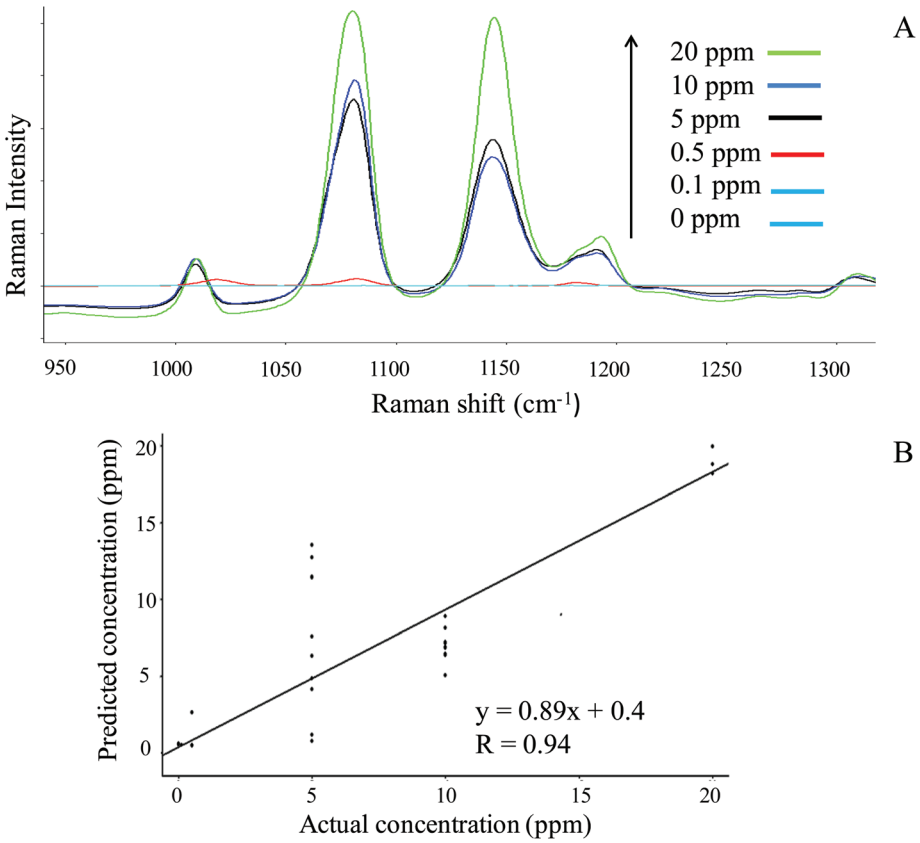

Fig. 3 SERS spectra of different concentrations (0–20 ppm) of 20 nm Ag NPs with PATP (A); a linear relationship between the predicted concentration and the actual concentration of Ag NPs (B).

netic enhancement at the junction between them.[43,44] Njoki and others observed that the correlation of the surface plasmon resonance band with the particle size of gold nanoparticles (10–100 nm diameters) is a key factor that is responsible for the SERS effect of the nanoparticles in solution.[45] This is in general agreement with our results that the range of 20–100 nm seemed to be the suitable size for SERS detection.

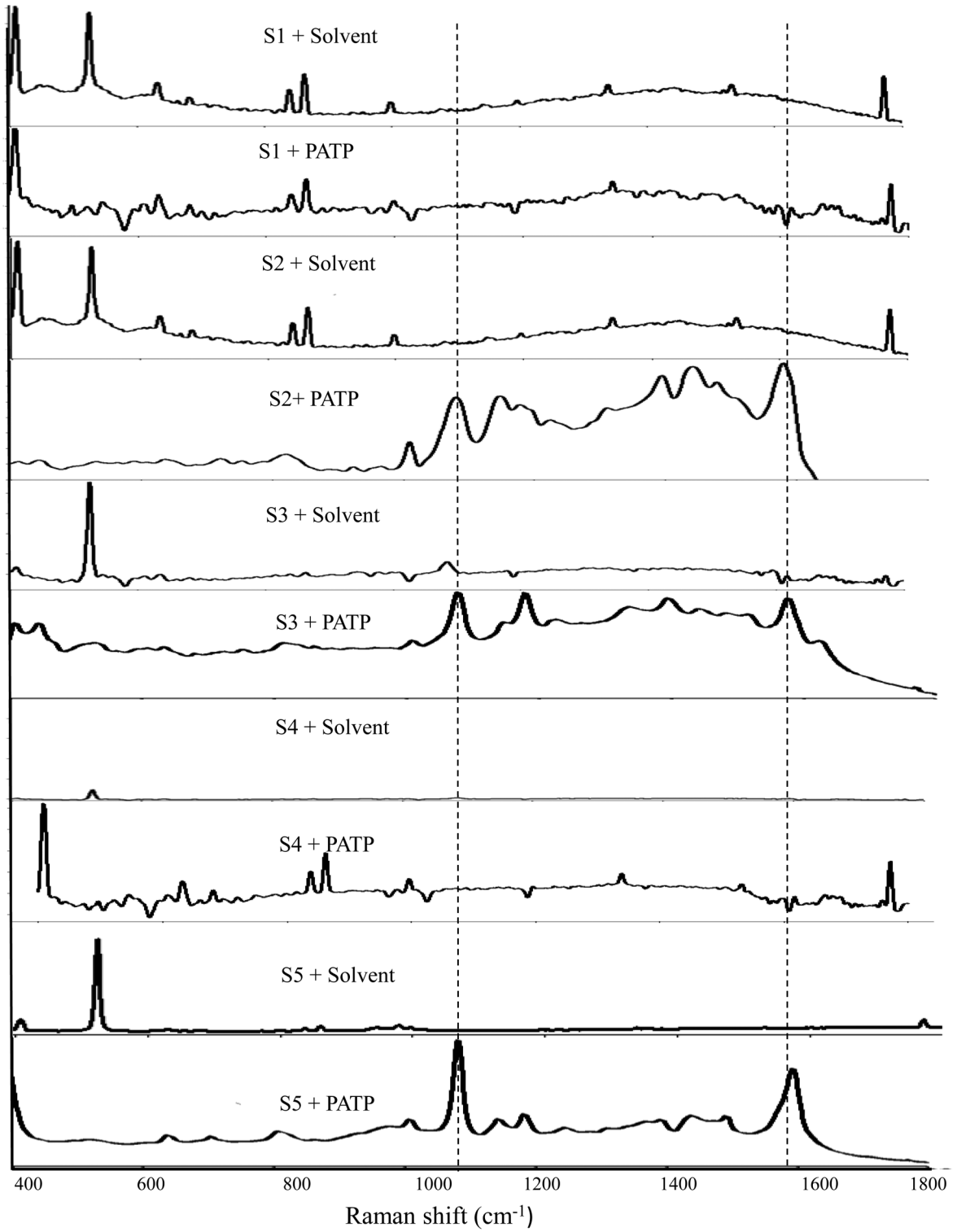

Fig. 4 SERS spectra of five Ag NP-containing dietary and antimicrobial products. Negative controls were prepared using the solvent of PATP (methanol).

Quantification of Ag NPs by SERS

In addition, we studied the reliability of the SERS method for the characterization and quantification of Ag NPs. Fig. 3A shows the average SERS spectra of samples with a concentration range of 0–20 ppm of 20 nm Ag NPs. A linear calibration curve was constructed by monitoring the intensity of the peaks in a selected region (400–1800 cm^{-1}). PLS analysis was conducted to obtain the RMSEP values from the PLS models. The lowest RMSEP value was achieved and used to construct the PLS prediction model. Fig. 3B illustrates the plot between the predicted concentrations and actual concentrations of Ag NPs (R = 0.94). Higher initial concentrations of Ag NPs resulted in more Ag NPs in the Ag NP–PATP complexes that were associated with additional PATP molecules. The LOD of Ag NPs of the method was calculated (~11 ppm) based on the aforementioned equation. The whole process of SERS measurement can be finished within one hour. These results demonstrate that a SERS method coupled with PLS can be used as a reliable method to quantify Ag NPs.

To further evaluate the SERS method for the quantification of Ag NPs, we established a linear calibration curve between the concentration of Ag NPs and the Raman intensity of a strong peak at 1079 cm^{-1}. The SERS intensity variations at two characteristic peaks (1079 and 1143.9 cm^{-1}) of 20 nm Ag NPs are provided in the ESI (Fig. S1†). The variations of SERS intensity can be due to the aggregation of NPs and the deposition of multiple NP monolayers. This problem is addressed by performing spectral averaging throughout the samples. The linear relationship clearly demonstrates the potential of SERS in the analysis of Ag NPs in simple solutions (data not shown). However, it is likely that the Raman intensity of the conjugation of Ag NP–PATP can be affected by the complex matrix of the commercial products. These findings led us to investigate the feasibility of this method for the detection of Ag NPs in five commercial products. Fig. 4 shows that the spectra of negative controls (samples (S1 to S5) + solvent of PATP) were in low intensity and no distinctive peaks were observed. In contrast, prominent and distinctive peaks (1079, 1143, 1430, and 1594 cm^{-1}) of Ag NP–PATP complexes were produced by the products (S2, S3, and S5) after interacting with 10 mg L^{-1} of PATP. Less prominent but still detectable peaks (1079 and 1143 cm^{-1}) were also observed for S1 and S4 as shown in Table 1. Compared to the spectra of the Ag NP–PATP complexes, the spectra of the nasal spray (S2) show similar features, indicating that the matrices may have influence on the Raman signals and thus on the detection of Ag NPs. While the spectra of the dietary supplements were more affected by their natural matrices, the characteristic Raman signals of the Ag NP–PATP complexes were still clearly observed. However, the order of the silver concentration claimed as S3 > S2 = S4 > S1 = S5 was different from the total silver concentration measured based on the SERS intensity of the peaks at 1079 and 1143 cm^{-1} (S2 > S5 > S3 > S4 > S1). These discrepancies may come from the fact that not all silver in the products was nano-sized and those nanoparticles may not have the same size distribution.

TEM and ICP-OES analyses were conducted to validate the SERS method by analyzing the size and concentration of Ag NPs in the samples. The total silver concentration in five commercial products was determined by ICP-OES (Table 1). The measured results were different from the claimed concentrations on the label, except for the sample S5. The total silver concentration of sample S3 was ~121 ppm, which was higher than the claimed concentration on the label. The order of the claimed silver concentration (S3 > S2 = S4 > S1 = S5) was different from the total silver concentration measured by ICP-OES of the products (S3 > S2 > S5 > S1 > S4). As shown in Table 1, the concentrations of Ag NPs (<3 kDa) in the products were not in the same order as the SERS signal intensity. The concentrations of S2, S3, and S5 are higher than those of S1 and S4 based on the SERS intensity and ICP-OES measurement.

TEM was used to analyze the size distribution of Ag NPs (Fig. 5) to determine the potential effect of particle size on the SERS intensity. The average sizes of Ag NPs in S1, S2 and S3 were 54.6, 47.2, and 54.8 nm, respectively (Table 1), which is larger than that of S4 (30.8 nm) and S5 (34.3 nm). The size of Ag NPs of the products is in the range of 20–100 nm. It was observed that the closer the particle size to the optimum range (30–40 nm) for the enhancement of SERS signals, the higher the signal intensity. Thus, it is speculated that S2, S4, and S5 would produce stronger SERS intensity than S1 and S3 at the same concentrations of Ag NPs. Interestingly, sample S4 had a significant lower concentration of Ag NPs (0.1 mg L^{-1}) than the rest of the samples and thus its SERS signals were low as well, even though its size was very close to

Table 1 Total concentration of silver and Ag NPs, average size, and the intensity of SERS spectra acquired from five commercial products

Product	Claimed concentration of Ag (ppm) on the label	Total silver concentration (ppm)	Silver nanoparticle concentration (ppm) (<3 kDa)	SERS intensity at 1079 cm^{-1}	SERS intensity at 1143.9 cm^{-1}	Average size measured by TEM (nm)
S1	10	5	4.6	161	194	54.6
S2	30	17	16.2	101 061	100 277	47.2
S3	50	121	120	9545	8332	54.8
S4	30	0.4	0.1	260	259	30.8
S5	10	10	8.2	61 855	32 835	34.3

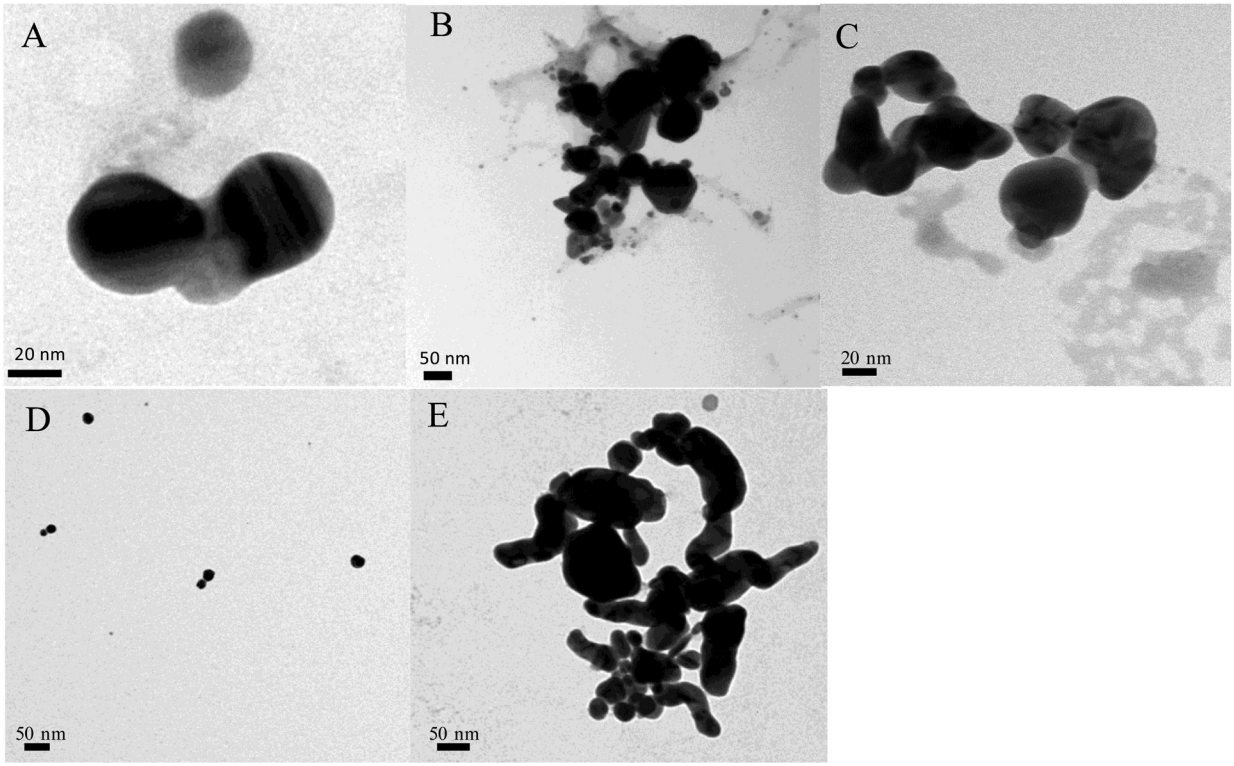

Fig. 5 Characterization of Ag NPs in the dietary supplements and antimicrobial products: (A) dietary supplement S1; (B) nasal spray S2; (C) dietary supplement S3; (D) dietary supplement S4; (E) dietary supplement S5.

the optimum range. These results demonstrate that TEM and ICP-OES can be used to validate SERS measurements that can reflect the size and concentration of Ag NPs in the consumer products.

Conclusions

A simple, fast, and effective SERS method was developed to detect and measure Ag NPs in commercial products. PATP can be used as a Raman indicator that binds strongly with Ag NPs. In this study, the feasibility of the SERS method was evaluated by measuring Ag NPs in four dietary supplements and one nasal spray with minimum sample preparation. The findings were validated by ICP-OES and TEM methods. These results demonstrate that there is great potential to use SERS for rapid detection and quantification of Ag NPs in consumer products. More research is needed to detect Ag NPs and other ENPs in various matrices.

Acknowledgements

We acknowledge the assistance from the Electron Microscopy Core facility at the University of Missouri in electron microscopy analysis. This research was supported by the University of Missouri Research Board and the USDA NIFA Nanotechnology Program (2011-67021-30391).

References

1 R. Y. Yada, N. Buck, R. Canady, C. DeMerlis, T. Duncan, G. Janer, L. Juneja, M. Lin, D. J. McClements, G. Noonan, J. Oxley, C. Sabliov, L. Tsytsikova, S. Vázquez-Campos, J. Yourick, Q. Zhong and S. Thurmond, *Compr. Rev. Food Sci. Food Saf.*, 2014, **13**, 730–744.
2 C. Marambio-Jones and E. M. Hoek, *J. Nanopart. Res.*, 2010, **12**, 1531–1551.
3 A. Sirelkhatim, S. Mahmud, A. Seeni, N. H. M. Kaus, L. C. Ann, S. K. M. Bakhori, H. Hasan and D. Mohamad, *Nano-Micro Lett.*, 2015, **7**, 219–242.
4 P. Arora, A. Sindhu, N. Dilbaghi and A. Chaudhury, *Biosens. Bioelectron.*, 2011, **28**, 1–12.
5 H. Sharma and R. Mutharasan, *Sens. Actuators, B*, 2013, **183**, 535–549.
6 R. K. Shukla, A. Kumar, A. K. Pandey, S. S. Singh and A. Dhawan, *J. Biomed. Nanotechnol.*, 2011, **7**, 100–101.
7 W.-S. Cho, M. Cho, J. Jeong, M. Choi, H.-Y. Cho, B. S. Han, S. H. Kim, H. O. Kim, Y. T. Lim and B. H. Chung, *Toxicol. Appl. Pharmacol.*, 2009, **236**, 16–24.
8 E.-J. Park, J. Yi, Y. Kim, K. Choi and K. Park, *Toxicol. in Vitro*, 2010, **24**, 872–878.
9 N. Asare, C. Instanes, W. J. Sandberg, M. Refsnes, P. Schwarze, M. Kruszewski and G. Brunborg, *Toxicol.*, 2012, **291**, 65–72.

10 Anon., The Project of Emerging Nanotechnologies, http://www.nanotecproject.org, (accessed April 15, 2016).
11 S. W. Wijnhoven, W. J. Peijnenburg, C. A. Herberts, W. I. Hagens, A. G. Oomen, E. H. Heugens, B. Roszek, J. Bisschops, I. Gosens and D. Van De Meent, *Nanotoxicology*, 2009, **3**, 109–138.
12 T. V. Duncan, *J. Colloid Interface Sci.*, 2011, **363**, 1–24.
13 R. J. Vandebriel and W. H. De Jong, *Nanotechnol., Sci. Appl.*, 2012, **5**, 61.
14 J. H. Sung, J. H. Ji, K. S. Song, J. H. Lee, K. H. Choi, S. H. Lee and I. J. Yu, *Toxicol. Ind. Health*, 2011, **27**, 149–154.
15 R. Podila and J. M. Brown, *J. Biochem. Mol. Toxicol.*, 2013, **27**, 50–55.
16 O. Lozano, J. Mejia, T. Tabarrant, B. Masereel, J.-M. Dogné, O. Toussaint and S. Lucas, *Anal. Bioanal. Chem.*, 2012, **403**, 2835–2841.
17 J. Falandysz, K. Szymczyk, H. Ichihashi, L. Bielawski, M. Gucia, A. Frankowska and S.-I. Yamasaki, *Food Addit. Contam.*, 2001, **18**, 503–513.
18 A. Ikem, A. Nwankwoala, S. Odueyungbo, K. Nyavor and N. Egiebor, *Food Chem.*, 2002, **77**, 439–447.
19 K. Loeschner, J. Navratilova, C. Købler, K. Mølhave, S. Wagner, F. von der Kammer and E. H. Larsen, *Anal. Bioanal. Chem.*, 2013, **405**, 8185–8195.
20 G. Singh, C. Stephan, P. Westerhoff, D. Carlander and T. V. Duncan, *Compr. Rev. Food Sci. Food Saf.*, 2014, **13**, 693–704.
21 Z. Zhang, F. Kong, B. Vardhanabhuti, A. Mustapha and M. Lin, *J. Agric. Food Chem.*, 2012, **60**, 10762–10767.
22 J. A. Gallego-Urrea, J. Tuoriniemi and M. Hassellöv, *Trends Anal. Chem.*, 2011, **30**, 473–483.
23 J. P. Helsper, R. J. Peters, L. Brouwer and S. Weigel, *Anal. Bioanal. Chem.*, 2013, **405**, 1181–1189.
24 D. Drescher, C. Giesen, H. Traub, U. Panne, J. Kneipp and N. Jakubowski, *Anal. Chem.*, 2012, **84**, 9684–9688.
25 Z. Zhang, Q. Yu, H. Li, A. Mustapha and M. Lin, *J. Food Sci.*, 2015, **80**, N450–N458.
26 A. Ahmed and R. Gordon, *Nano Lett.*, 2012, **12**, 2625–2630.
27 K. Kneipp, H. Kneipp, V. B. Kartha, R. Manoharan, G. Deinum, I. Itzkan, R. R. Dasari and M. S. Feld, *Phys. Rev. E: Stat. Phys., Plasmas, Fluids, Relat. Interdiscip. Top.*, 1998, **57**, R6281.
28 K. Kneipp, Y. Wang, H. Kneipp, L. T. Perelman, I. Itzkan, R. R. Dasari and M. S. Feld, *Phys. Rev. Lett.*, 1997, **78**, 1667.
29 Y. Zhang, W. Yu, L. Pei, K. Lai, B. A. Rasco and Y. Huang, *Food Chem.*, 2015, **169**, 80–84.
30 F. Zhai, Y. Huang, C. Li, X. Wang and K. Lai, *J. Agric. Food Chem.*, 2011, **59**, 10023–10027.
31 X. Song, H. Li, H. Al-Qadiri and M. Lin, *J. Food Measurement Characterization*, 2013, **7**, 107–113.
32 X. Hu, T. Wang, L. Wang and S. Dong, *J. Phys. Chem. C*, 2007, **111**, 6962–6969.
33 Y.-F. Huang, D.-Y. Wu, H.-P. Zhu, L.-B. Zhao, G.-K. Liu, B. Ren and Z.-Q. Tian, *Phys. Chem. Chem. Phys.*, 2012, **14**, 8485–8497.
34 K. Kim, H. B. Lee, J. K. Yoon, D. Shin and K. S. Shin, *J. Phys. Chem. C*, 2010, **114**, 13589–13595.
35 Y. Wang, X. Zou, W. Ren, W. Wang and E. Wang, *J. Phys. Chem. C*, 2007, **111**, 3259–3265.
36 J. Zheng, Y. Zhou, X. Li, Y. Ji, T. Lu and R. Gu, *Langmuir*, 2003, **19**, 632–636.
37 T. H. Nguyen, Z. Zhang, A. Mustapha, H. Li and M. Lin, *J. Agric. Food Chem.*, 2014, **62**, 10445–10451.
38 H. Martens and T. Naes, *Multivariate calibration*, John Wiley & Sons, 1992.
39 M. Lin, A. G. Cavinato, Y. Huang and B. A. Rasco, *Food Res. Int.*, 2003, **36**, 761–766.
40 B. Liu, P. Zhou, X. Liu, X. Sun, H. Li and M. Lin, *Food Bioprocess Technol.*, 2013, **6**, 710–718.
41 M. Moskovits, *J. Raman Spectrosc.*, 2005, **36**, 485–496.
42 C. S. Seney, B. M. Gutzman and R. H. Goddard, *J. Phys. Chem. C*, 2009, **113**, 74–80.
43 Z. Lu, W. Ruan, J. Yang, W. Xu, C. Zhao and B. Zhao, *J. Raman Spectrosc.*, 2009, **40**, 112–116.
44 C. J. Orendorff, A. Gole, T. K. Sau and C. J. Murphy, *Anal. Chem.*, 2005, **77**, 3261–3266.
45 P. N. Njoki, I.-I. S. Lim, D. Mott, H.-Y. Park, B. Khan, S. Mishra, R. Sujakumar, J. Luo and C.-J. Zhong, *J. Phys. Chem. C*, 2007, **111**, 14664–14669.